1st Croatian Conference on Earthquake Engineering
1CroCEE
22-24 March 2021 Zagreb, Croatia

DOI: https://doi.org/10.5592/CO/1CroCEE.2021.136

Fragility analysis of rc building with the application of nonlinear analysis

Radomir Folić[1], Miloš Čokić[2]

[1] *Professor Emeritus*, University of Novi Sad, Faculty of Technical Sciences, Serbia, *folic@uns.ac.rs, r.folic@gmail.com*

[2] *PhD student*, University of Novi Sad, Faculty of Technical Sciences, Serbia, *cokicmilos@gmail.com*

Abstract

In this paper, the seismic response of a 5 story reinforced concrete (RC) frame system building is analysed through the fragility analysis. The construction is designed in accordance with structural Eurocodes: EN1990; EN1991; EN1992; EN1998, as a ductility class high (DCH) system. For the analysis of the response of structural system to the earthquake actions, the methods of nonlinear static (NSA) and nonlinear dynamic analyses (NDA) were applied and, based on the obtained results, fragility curves were constructed using statistical methods. Fragility curves are functions of intensity measure (IM) and engineering demand parameter (EDP). Fragility functions represent a possibility for different states of damage to occur in certain structural system, at observed value of specified IM. Pushover analysis was performed as a part of NSA and time history (TH) procedure was used as a part of incremental NDA. Ten accelerograms, used in NDA, are selected and scaled according to EN1998 provisions, for the chosen elastic response spectrum and referent PGA. Obtained results were used for the statistical analysis and construction of fragility curves. Structural damage state threshold parameters are determined based on the methodologies described by Park and Ang and in FEMA, HAZUS and EN codes. Comparative analysis of the structural damage probability for the analysed RC building, calculated using different methodologies to determine damage states, is applied. Based on the analysis results, final remarks and conclusions were formulated.

Key words: RC building, seismic nonlinear analyses, fragility, FEMA, Eurocode, HAZUS, Damage index

1 Introduction

In the domain of seismic engineering, fragility function can be used to calculate the possibility for different states of damage to occur in certain construction, at observed value of intensity measure. According to [1], one can define a fragility function as a mathematical function that expresses the probability that some undesirable event occurs as a function of some measure of environmental excitation. Fragility function represents the cumulative distribution function of the capacity of an asset to resist an undesirable limit state.

In this paper, fragility curves for different types of damage (in term of severity) are functions of intensity measure (*IM*) represented through values of peak ground acceleration (*PGA*) and engineering demand parameter (*EDP*) which is represented through the response of the analysed construction. The limit state (*LS*) values used in this paper as *EDP*, for determination of structural damage, are functions of inter-story drifts (*IDR*) [2, 3], damage index (*DI*) [4], and *PGA* [5, 6]. Seismic structural response is analysed through nonlinear pushover and time history analysis (*THA*), using the incremental non-linear static analysis (*INDA*) method. Fragility curves were constructed using mathematical statistic and probability methods, based on the obtained results and *IM-EDP* relationship.

In this paper, fragility curves are calculated for a 5 story reinforced concrete (RC) building that exhibits the properties of the frame structural system [5]. The structural system was designed according to set of structural Eurocodes [5, 7, 8, 9]. Based on the analysis, obtained results are compared and final remarks and conclusions were formulated.

2 Methodology of the analysis and structural modelling

2.1 Geometric and material properties of the structure

The subject of the analysis is office-residential building (Fig. 1) with 5 levels (ground floor+4 stories). The structural system exhibits the properties of a frame structural system [5]. The plan view and the 3D model of the structure are shown in Figure 1. The length of one span in both directions is 4.8 m which makes the total length of the building 19.2 m in both directions. The height of the first story is 3.6 m and the height of the other stories is 3.2 m which makes the total height of the building 16.4 m. In order to simplify the modelling and calculation process, all vertical elements are fixed at the bottom level of the structure, i.e. soil-structure interaction is not included in the calculation and design.

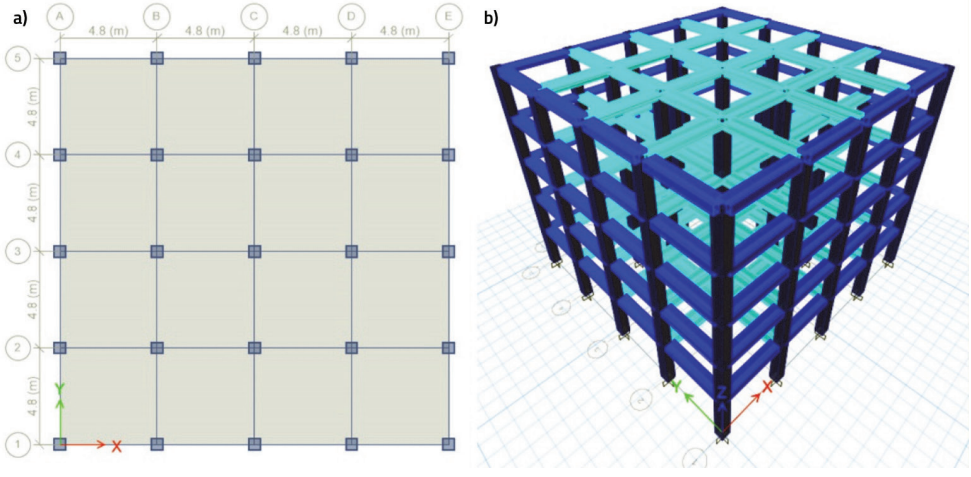

Figure 1. a) Building plan; b) Numerical model

The design of the structure is done according to the recommendations given in the set of structural Eurocodes [5, 7, 8, 9] using linear-elastic analysis methods. Material properties of concrete *C35/45* and reinforcing steel class *C* (f_{yk} = 500 MPa, E_y = 200 GPa) [9] have been adopted for model analysis.

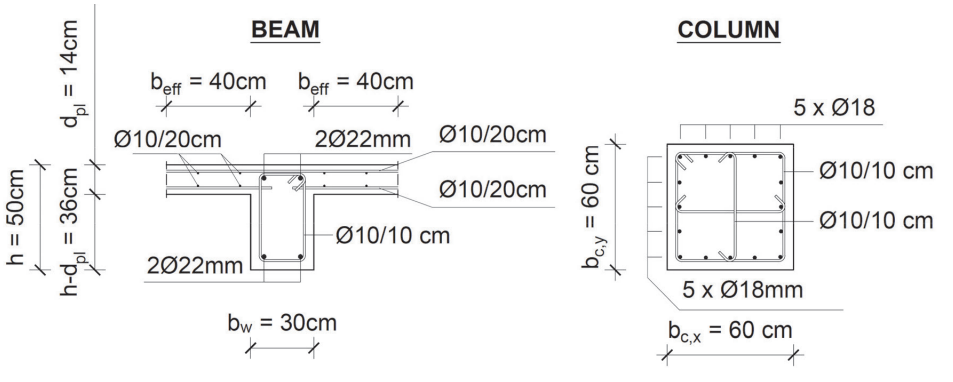

Figure 2. Geometric and reinforcement characteristics of the cross-section properties of the beams (left) and columns (right)

The structural design is done according to the European building design standards, for the structure that has ductility class high (*DCH*) behaviour [5]. The calculations are performed using [10]. Geometric and reinforcement characteristics of the cross-section properties of the beams and columns are shown in Fig. 2.

2.2 Loads and actions

The loads acting on the structure are as follows: permanent loads (G_i) – self-weight of structural elements and an additional permanent load; the variable-live load (Q_i) and the seismic load (S_i). The adopted value of the permanent constant load is g_{pl} = 3.0 kN/m^2 and the load intensity of the variable-live load amounts q = 2.0 kN/m^2 on all floors except the roof, where it amounts q_R = 1.0 kN/m^2. The self-weight load of façade elements, which is imposed on all façade elements except on the roof is equal to g_f = 10.0 kN/m. The value of the reduction factor of the live loads is $\psi_{2,i}$ = 0.3 [8]. To calculate the earthquake impact on the structure, an elastic response spectrum, type 1 was used, for ground type C, with the *PGA* a_g = 0.2g. Behaviour factor q of the design response spectrum for a frame structural system is equal to 5.85 [5].

2.3 Modal analysis

Modal analysis was performed to determine the fundamental periods of vibrations of the system, modes (Fig. 3) and system rigidity or flexibility [5]. It is established that the system is torsionally rigid and that translational modes are dominant. *Rayleigh* viscous (mass – tangent stiffness) proportional damping was used in *THA*. An overview of modern seismic analyses with different damping models is explained in [11]. The appropriate values of periods of vibration in both directions for T_1 correspond to the first translation period in X or Y direction (the structure is orthogonal in the plane and its behaviour will be the same in the both main directions). The value of T_2 corresponds to the period of vibration in which the structure reaches at least 90 % of the sum of the effective modal masses [5]. Values of the used periods are T_1 = 0.735 s (80.41 % mass), T_2 = 0.213 s (92.69 % mass in sum).

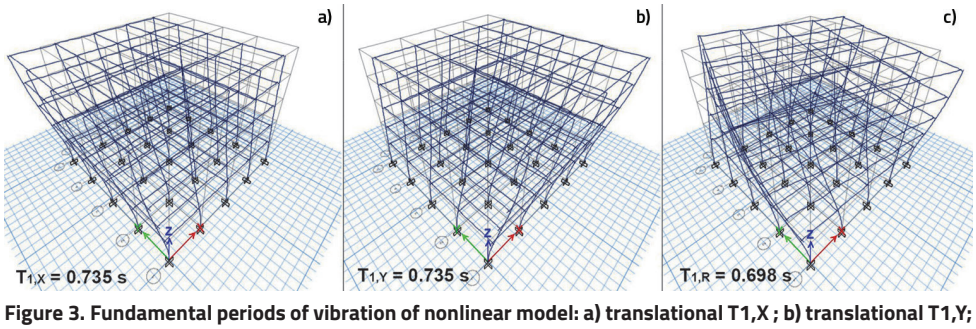

Figure 3. Fundamental periods of vibration of nonlinear model: a) translational T1,X ; b) translational T1,Y; c) rotational T1,R

2.4 Nonlinear dynamic analysis

THA is conducted by using ten particular accelerograms in only one direction at the time and not by combining their *N-S*, *W-E* and vertical components for 3-directional analysis, because of its simplicity and wide application of this method of analysis. The accelerograms were chosen from [12, 13] and scaled according to elastic response spectrum for the intensity level of 10 % of possibility of exceedance in 50 years (Fig. 4).
EQ01-EQ06 are selected from [12] and *EQ07-EQ10* are selected from [13]. The criteria for time-history data selection was that magnitude M>5.*5Ms* (Type 1 RS [5]), the records correspond to soil Type C and $v_{s,30}$ = 180 – 360 m/s [5]. In addition, records from [13] are obtained using *REXELite* tool that allows searching for a suite of waveforms compatible with a target spectrum, generated according to [5]. According to [5] the conditions $S_{a,\mu}^{scaled}(T_0) \geq a_g \cdot S$ and $S_{a,\mu}^{scaled} \geq 0.9 \cdot S_{a,EC8}^{Elastic}$ on the interval of $[0.2 \cdot T_1 - 2 \cdot T_2]$ are satisfied (Fig. 4). Selected earthquake data is shown in Table 1. *THA* data was scaled (Fig. 4) with the common scale factor F_S = 1.61, which was obtained using the least square method (*LSM*). The whole procedure is very detailed described in [14, 15]. Scaled accelerograms are used for *INDA*, with the increment of Δ*PGA* = 0.1*g*, in total scaling factor range of 0.1*g* – 1.0*g*.

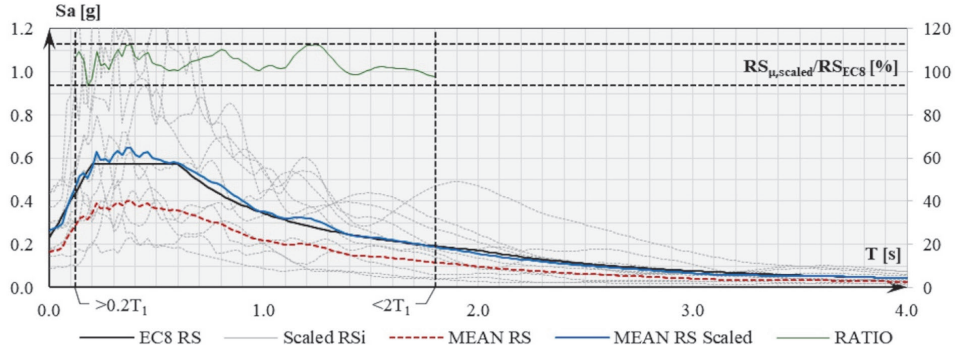

Figure 4. Response spectrums used in the analysis (scaled RS_i, mean RS and mean scaled RS)

Table 1. Main properties of the earthquakes that were used in NDA

ID	Earthquake location	Earthquake ID (component/orientation)	Station ID/ Code	Date/Time	M_w	Original PHA [cm/s^2]
EQ01	Spitak, Armenia	213 (Y)	173	07/12/1988 07:41:24	6.7	179.580
EQ02	Manjil, Western Iran	230 (Y)	189	20/6/1990 21:00:08	7.4	87.045
EQ03	Umbria Marche, Central Italy	286 (Y)	221	26/9/1997 09:40:30	6.0	218.340
EQ04	Umbria Marche, Central Italy	286 (Y)	224	26/9/1997 09:40:30	6.0	106.660
EQ05	Alkion, Greece	559 (X)	214	15/6/1995 00:15:51	6.5	55.501
EQ06	Düzce, Turkey	497 (Y)	3139	12/11/1999 16:57:20	7.2	112.320
EQ07	Umbria, Central Italy	EMSC-20161030_0000029 (N-S)	CNE	30/10/2016 06:40:18	6.5	288.280
EQ08	Emilia-Romagna, Italy	IT-2012-0011 (N-S)	MOG0	29/5/2012 07:00:02	6.0	167.075
EQ09	Adana, Turkey	TK-1998-0063 (E-W)	0105	27/6/1998 13:55:53	6.2	271.955
EQ10	Emilia-Romagna, Italy	IT-2012-0011 (N-S)	MIR08	29/5/2012 07:00:02	6.0	242.970

3 Structural model

3.1 Model for linear-elastic analysis

For calculation and design of the structure in [10], a spatial (3D) model was used. The following parameters, assumptions and simplifications were adopted:

- The calculation includes the effects of second order logic (*P*-Δ);
- Occurrence of cracks in structural elements was included in the calculation with the stiffness reduction of the elements according to [5].
- The elastic bending stiffness and shear stiffness of columns and beams was reduced to 50 %;
- Torsion stiffness of columns and beams was reduced to 10 % of their elastic stiffness;
- The elastic bending stiffness of the RC plate was reduced to 50 %.

3.2 Model for nonlinear analysis

In models for post-elastic analysis of structural response to the removal of individual vertical elements, the following assumptions and simplifications were used:

- The calculation includes the effects of second order logic (*P*-Δ);
- To describe the nonlinear behaviour of the material, the nonlinear properties of the material were used to describe the behaviour of concrete (Fig. 5) and reinforcement steel [9, 16, 17];
- Parameters describing the appearance of cracks as a result of elastic bending stiffness in structural elements from the linear-elastic model were not included in the nonlinear model, because plastic hinges are modelled as fiber elements, whereas the properties of fibers are described by stress-strain relations in concrete and reinforcement steel (Fig. 5);
- Columns and beams were modelled as confined RC elements with a protective layer of concrete [16];
- The beams are modelled as "*L*" and "*T*" cross sections, with the effective width of the RC plate.
- RC plates are modelled as rigid diaphragms.

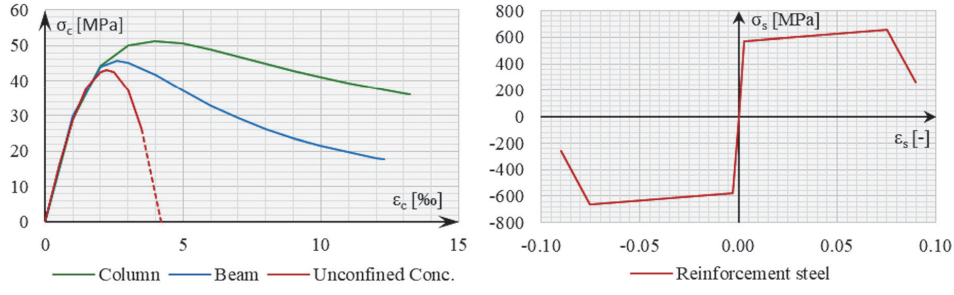

Figure 5. Material properties of concrete (left) and rebar (right)

3.3 Properties of plastic hinges

Plastic hinges are modelled as fiber cross sections. They are modelled by automatic selection of fiber division in the cross section of elements [10]. Among many expressions for the calculation of plastic hinge length [18] and because of the inconsistency among the values obtained by different expressions, the equations suggested by [19] and [20] are the most practical for the modelling and the analysis. It is estimated that the lengths of plastic hinges, calculated according to [19] and [20] correspond approximately to the relative lengths of columns and beams of 0.1*L*, where *L* is the length of the element. Therefore, the locations of the hinges are assigned as 0.05*L* and 0.95*L* to columns and beams in [10]. Behaviour of the fiber plastic hinges used in the calculations is a function of auto-discretised group of fibers and their stress-strain relationship for the materials which are used in the formation of the structure's cross-sections (Fig. 6).

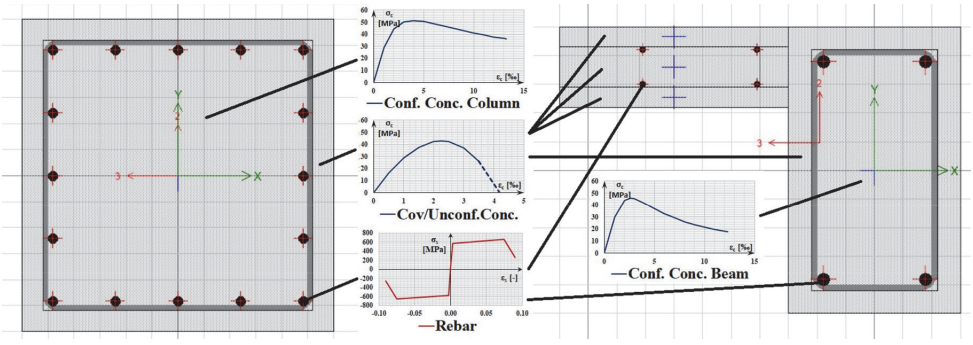

Figure 6. Schematic representation of column (left) and *L* beam (right) auto-discretised sections with appropriate stress-strain properties depending on material used)

4 Non-linear analysis results and calculation of fragility curves

4.1 INDA analysis

The results of *NSA* for mass-proportional and modal load distributions and *INDA* are shown in Fig. 7. Modal pushover curve has a better fit to *INDA* values, so it was chosen as a referent curve for the calculation of fragility curves, using DI_{PA} as *EDP*, according to [4]. To perform the calculation of DI_{PA}, it was necessary to do an bilinear approximation of *NSA* pushover curve, using Equivalent Energy Elastic-Plastic (*EEEP*) method and determine yielding (d_Y,F_Y) = (8.03 cm, 8235.59 kN) and ultimate capacity (d_U,F_U) = (31.86 cm, 8235.59 kN) points. Displacement (*d*), *IDR* and their mean values in arithmetic space for lognormal distribution, obtained using *INDA* are displayed in Fig. 8.

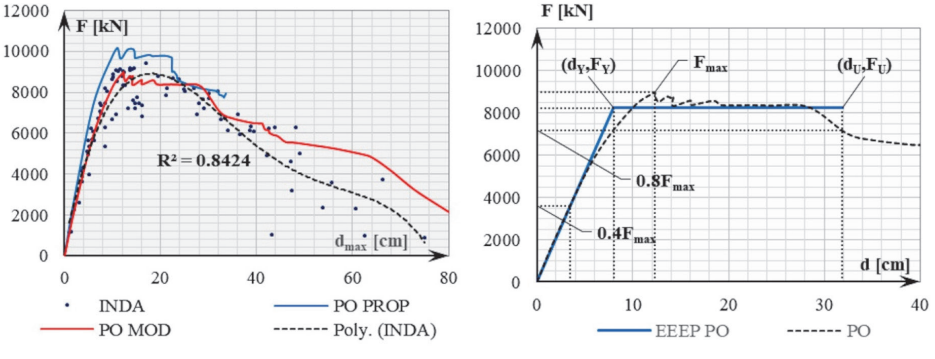

Figure 7. *NSA* and *INDA* results (left) and pushover curve bilinear approximation (right)

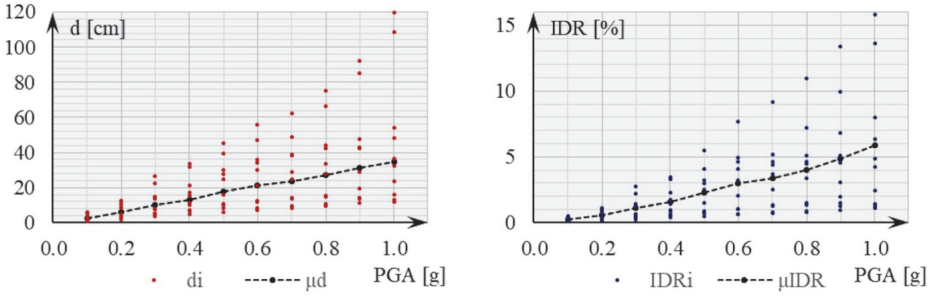

Figure 8. Roof displacement (left) and *IDR* results (right) obtained using *INDA*

4.2 Damage state performance points

Damage of a structural system may be quantified through threshold performance points, which represent the values of *EDP*, which are obtained by *NSA* and *INDA* in this paper. There are several methods to define damage state performance points. The ones described in [2-6] were used to calculate fragility curves. *Park* and *Ang* damage index [4] for structural damage (DI_{PA}) is calculated according to following formula:

$$DI_{PA} = \frac{d_M}{d_U} + \beta \cdot \frac{1}{Q_Y \cdot d_U} \cdot \int dE \tag{1}$$

Where d_M represents maximum deformation under earthquake in *THA*, d_U ultimate deformation capacity under monotonic loading; Q_Y yield strength under monotonic loading; *dE* incremental absorbed hysteretic energy during the earthquake and β is non-negative parameter representing the effect of cyclic loading on structural damage, usually equal to 0.15 for RC structures [21].

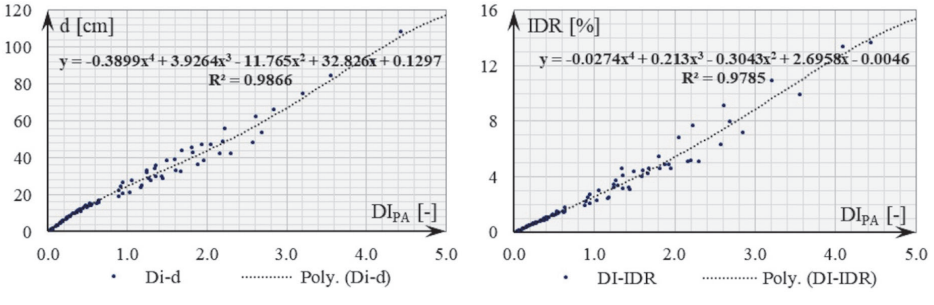

Figure 9. *DI*, DI_{mod1}, DI_{mod2} (left) and their comparison to referent *DI* (right)

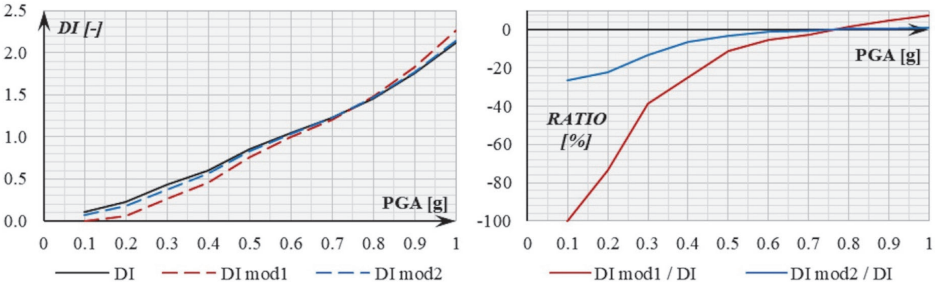

Figure 10. Relationship between DI_{PA} – d and DI_{PA} – IDR

Modified *Park* and *Ang* damage index [4], proposed by [22] is calculated by the following equation:

$$DI_{PA} = \frac{D_M - D_Y}{D_U - D_Y} + \beta \cdot \frac{1}{F_Y \cdot D_U} \cdot \int_{E(t=0)}^{E(t=n)} dE \geq 0 \text{ (if } F_U < F_Y,\ F_Y \text{ is replaced by } F_U) \quad (2)$$

Where D_M represents the maximum roof displacement under earthquake in THA, D_U ultimate roof displacement on bilinearized pushover curve (Fig. 7, right); F_Y yield roof displacement on bilinearized pushover curve (Fig. 7, right); $\int_{E(t=0)}^{E(t=n)} dE$ absorbed hysteretic energy during the earthquake (from $t = 0$ to $t = n$, where n is the last integration point of the accelerogram). An alternative value for D_Y may be taken as the first yield displacement from *THA*, at the point of first non-zero value of E_h. Modified DI_{PA} with D_Y value from the bilinearized pushover curve (DI_{mod1}) and with D_Y value from THA (DI_{mod2}) are compared to the original DI_{PA} (eq.) and it is concluded that the DI_{mod2} has much better fit. More accurate and complex modified *DI* model was proposed and discussed in [21]. The calculated values and their comparation to DI_{PA} (eq. 2) are shown in Fig. 9.

DI_{PA} from the (eq. 1) is chosen for the fragility analysis because it will give the values on the safety side. Relation between performance points threshold and *EDP* values are given in Table 2. After the values of DI_{PA} were calculated, it was possible to find a relationship between d and DI_{PA} and also *IDR* and DI_{PA} (Fig. 10) using regression analysis in [23]. In that way, it was possible to compare damage state thresholds through different *EDP* parameters (Table 2).

In terms of the severity of the structural damage, structural damage states are defined as:

- FEMA: *IO* – immediate occupancy; *LS* – life safety; *CP* – collapse prevention [2],
- EN1998: *DL* – damage limitation; *SD* – significant damage; *NC* – near collapse [5, 6],
- DI_{PA} and HAZUS: *SD* – small damage; *MD* – moderate damage; *ED* – extensive damage; *CD* – complete damage [3, 4].

Table 2. Structural damage state threshold values, according to [2, 3, 4, 5, 6]

FEMA	**IO**		**LS**		**CP**	
IDR [%]	1		2		4	
EN	**DL**		**SD**		**NC**	
	0.794		1		1.710	
$\mathbf{PGA_g^{DS}}$ [g]	γ_{DL} PGA_{EL} = 0.159		γ_{SD} PGA_{EL} = 0.2		γ_{NC} PGA_{EL} = 0.342	
Damage Index	**SD**	**MD**		**ED**		**CD**
DI [-]	0.1	0.25		0.4		1
IDR [%]	0.262	0.654		1.038		2.573
HAZUS	**SD**	**MD**		**ED**		**CD**
IDR [%]	0.333	0.6		1.533		4

4.3 Statistical analysis of the results

It is generally assumed that fragility curve is a lognormal distribution function, which means that "*If a variable is lognormally distributed, its natural logarithm is normally distributed. Which means it must take on a positive real value, and the probability of it being zero or negative is zero.*" [1] Using *Kolmogorov-Smirnov* and *Anderson-Darling* tests in [24] on the results obtained through *INDA* method, it is established that for each *IM* and *EDP* distribution, the values fit the lognormal distribution. That also means that the relationship between ln(*IM*) and ln(*EDP*) has normal distribution for each ln(IM) in log-log space (*l.l.s.*). If each probability density function (*PDF*) in log-log space can be described as $Y \sim N(\mu, \sigma^2)$ and each *PDF* in arithmetic space (*a.s.*) as $X \sim \ln N(\mu, \sigma^2)$, conversion of *l.l.s.* values to *a.s.* can be performed by following expressions:

$$m_{a.s.} = e^{\left(\mu_{l.l.s.} + \frac{1}{2}\cdot\sigma^2_{l.l.s.}\right)};\ \mu_{a.s.} = e^{\left(\mu_{l.l.s.}\right)};\ \sigma^2_{a.s.} = \left|e^{\sigma^2_{l.l.s.}} - 1\right| \cdot e^{\left(2\cdot\mu_{l.l.s.} + \sigma^2_{l.l.s.}\right)} \tag{3}$$

Where $m_{a.s}$, $\mu_{a.s}$ and $\sigma_{a.s}$ represent the mean, median and the standard deviation value of the variable in arithmetic space and $\mu_{1.1.s}$ represent the mean and median value and $\sigma_{1.1.s}$ represent the standard deviation value of the variable in the log-log space.

4.4 Calculation of fragility curves

Since it is established that for each distribution of *IM* or *EDP*, values fit the lognormal distribution, probability density function (*PDF*) will be expressed with the equation:

$$f^{IM}_{LN,DS_i} = \frac{1}{x}\cdot\frac{1}{\sigma^{IM}_{LN|DS_i}\cdot\sqrt{2\pi}}\cdot e^{\frac{\left(\ln IM - \mu^{IM}_{LN|DS_i}\right)^2}{2\cdot\sigma^{IM\ 2}_{LN|DS_i}}} \tag{4}$$

where $\mu^{IM}_{LN|DS_i} = \mu^{IM}_{l.l.s.,i}$ and $\sigma^{IM}_{LN|DS_i} = \sigma^{IM}_{l.l.s.,i}$ represent the median and the standard deviation valueof the variable ln*IM* for eachdamage state (DS).
In case of the calculation of fragility curves, using *IM* as a referent value for the *DS* threshold [5, 6], the fragility function is calculated as analytical cumulative distribution function (*CDF*) for lognormal distribution:

$$P_{DS_i|IM}\left(\mu^{IM}_{LN|DS_i}, \sigma^{IM}_{LN|DS_i}\right) = \Phi\left(\frac{\ln IM - \mu^{IM}_{LN|DS_i}}{\sigma^{IM}_{LN|DS_i}}\right) \tag{5}$$

where Φ is the cumulative distribution function of the standard normal distribution. However, these fragility curves [5, 6] will be a functions of *DS* probability and *IM* = *IDR* or *IM* = *d* and not *IM* = *PGA*, which is characteristic for other *DS* fragility functions.

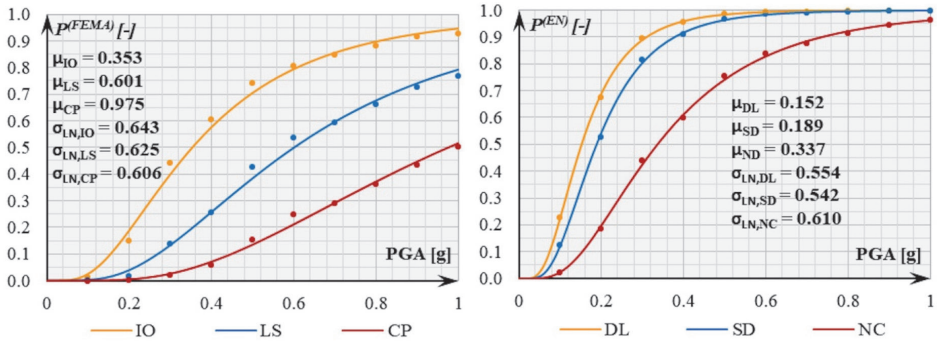

Figure 11. Fragility curves calculated according to FEMA [2] (left) and Eurocode [5, 6] (right) *DS* tresholds

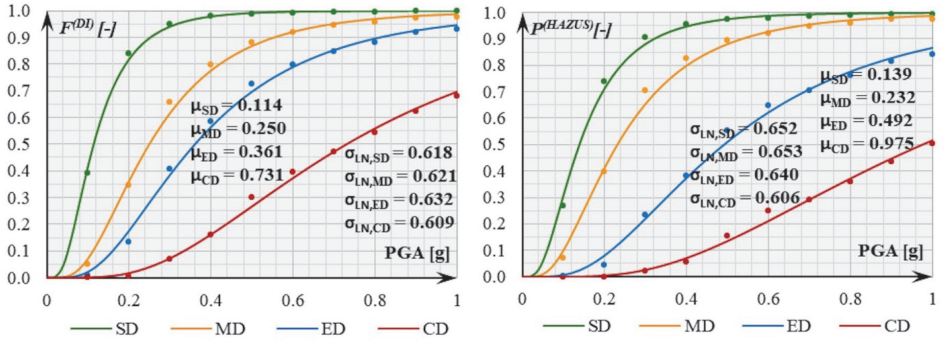

Figure 12. Fragility curves calculated according to *Park* and *Ang* [4] (left) and HAZUS [3] (right) *DS* thresholds

In case of the calculation of fragility curves, using *EDP* as a referent values, the probability of the occurrence of a defined damage state at a particular intensity measure value ($P_{DSi|IMj}$) can be calculated using the expression:

$$P_{DS_i|IM_j}\left(\mu^{EDP_i}_{LN,IM_j},\sigma^{EDP_i}_{LN|IM_j}\right)=1-\Phi\left(\frac{\ln EDP_i-\mu^{EDP_i}_{LN,IM_j}}{\sigma^{EDP_i}_{LN|IM_j}}\right) \tag{6}$$

where $\mu^{EDP_i}_{LN,IM_j}$ and $\sigma^{EDP_i}_{LN|IM_j}$ are mean and standard deviation in *I.l.s.* of *PDF* of the variable $\ln EDP_i$ for a particular $\ln IM_j$ value. $\ln EDP_i$ is the lognormal value of a *DS* threshold. These fragility curves are calculated using multiple stripe analysis (*MSA*) method [25]. Probability values are calculated at each IM_j for each DS_i. When all the probability values are calculated, the set of obtained points is fitted for each *DS*, by using maximum likelihood estimation (*MLE*) method [1, 25]. After applying *MLE*, we can obtain mean and standard deviation $\left(\mu^{IM}_{LN|DS_i},\sigma^{IM}_{LN|DS_i}\right)$ as a function of *IM*, for both log-log and arithmetic space. Because the relationship between *PGA* and *IDR* or *d* is calculated, the fragility curves for *DS* according to [5, 6] can now be converted to functions which have *PGA* as *IM*, using the described procedure. Calculated fragility curves are shown in Fig. 11 and Fig. 12. Probability density functions for the occurrence of different states of damage are calculated using the equations [1, 25]:

$$\begin{aligned}
P_{DS_0} &= 1-P_{DS_1}\left[IM_j,\mu_{LN|DS_1},\sigma_{LN|DS_1}\right]\\
P_{DS_i} &= P_{DS_i}\left[IM_j,\mu_{LN|DS_i},\sigma_{LN|DS_i}\right]-P_{DS_{i+1}}\left[IM_j,\mu_{LN|DS_{i+1}},\sigma_{LN|DS_{i+1}}\right]\\
P_{DS_n} &= P_{DS_n}\left[IM_j,\mu_{LN|DS_n},\sigma_{LN|DS_n}\right]
\end{aligned} \tag{7}$$

Where P_{DS0} is a probability of no damage to occur and i = 1, ..., n and IM_j = (0g-1.0g). i is an index of a particular *DS*, and j is an index of a particular *IM* (*PGA*). n is a total number of damage states.

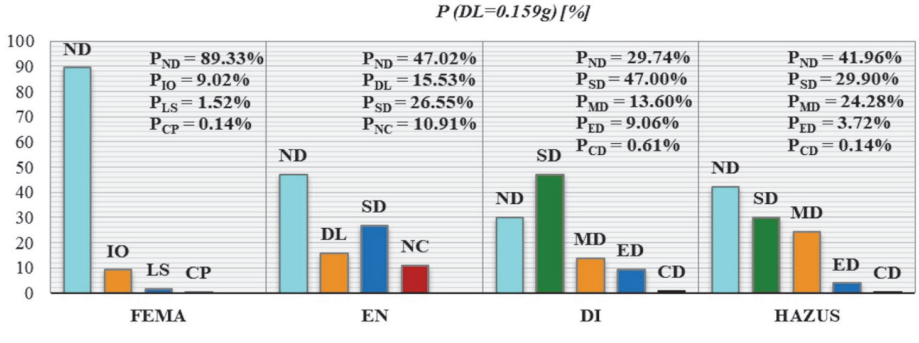

Figure 13. Probability for *DS* to occur at *PGA(DL)*

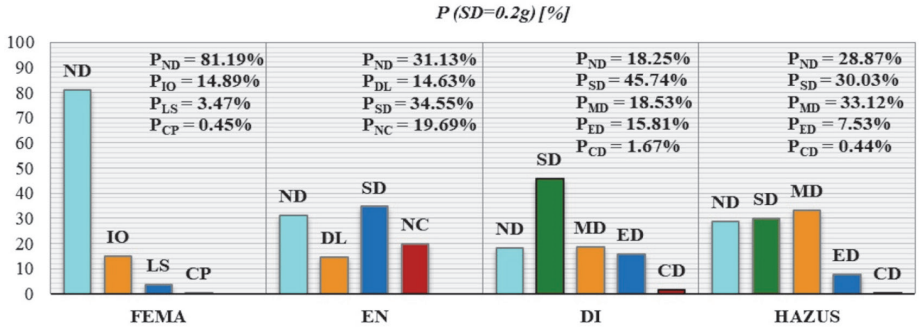

Figure 14. Probability for *DS* to occur at *PGA(SD)*

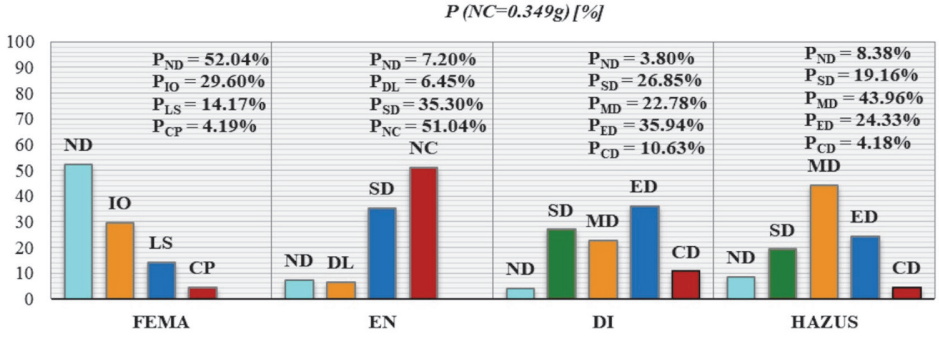

Figure 15. Probability for *DS* to occur at *PGA(NC)*

Probability of the occurrence of damage according to [2, 3, 4, 5, 6] is presented for the PGA at which the damage states *DL* (Fig. 13), *SD* (Fig. 14) and *NC* (Fig. 15) occur, according to [5, 6].

5 Discussion of the results

The analysis shows the difference between the results of the fragility analysis according to different DS thresholds. Fragility curves and *DS* occurrence probability calculated according to FEMA [2] will result in the least conservative values, opposing to the procedure according to Eurocodes [5, 6], which gives the results that are the most on the side of safety among all four procedures. Fragility curves and *DS* occurrence probability calculated according to *Park* and *Ang* [4] and HAZUS [3] give the similar results, but the values according to [4] are a bit more on the safety side.

6 Conclusions

In this paper, the comparative analysis of the seismic fragility of a RC frame structure, with damage state thresholds, calculated according to different codes [2-6] is per-

formed. The construction is designed as a *DCH* system, with behaviour factor q = 5.85. The system's fragility curves were derived from the results of *NSA* and *INDA*, using statistical methods. Different *EDP* values were selected for the assessment of damage states, while *PGA* was selected as the intensity measure *IM*. Probabilities of the occurrence of each *DS* for all mentioned codes are determined and compared.

Based on the comparative analysis, it can be concluded that based on the approach for determination of EDP values, according to different code, results may wary significantly in the range where it can be concluded that the structure is overstrengthened [2] or designed close to its full bearing capacities [5, 6] for design PGA. More descriptive and a bit more complex procedures described in [3] and [4], where the fragility results are related to *IDR* [4] and displacement and hysteretic energy [3] values are more in between the values obtained by [2] and [5, 6] and they give the most satisfying results in the fragility analysis.

Acknowledgements

The research described in this paper was financially supported by the Ministry of Education and Sciences of Republic of Serbia within the Project: "Multidisciplinary theoretical and experimental research in education and science in the fields of civil engineering, risk management and fire safety and geodesy." (University of Novi Sad, Faculty of Technical Sciences, Department of Civil Engineering and Geodesy). This support is gratefully acknowledged.

References

[1] Porter, K. (2015): "A Beginner's Guide to Fragility, Vulnerability, and Risk. University of Colorado Boulder", University of Colorado Boulder, DOI 10.1007/978-3-642-35344-4_256 (accessed: November 2020)

[2] FEMA356, ASCE, Prestandard and Commentary for the Seismic Rehabilitation of Buildings, November 2000

[3] Hazus®-MH 2.1, Earthquake Loss Estimation Methodology, Advanced Engineering Building Module (AEBM), Technical and User's Manual Developed by: Department of Homeland Security, FEMA, Mitigation Division, Washington, D.C.

[4] Park, Y.J., Ang, A.H.-S. (1985): Mechanistic seismic damage model for reinforced concrete, Journal of Structural Engineering, ASCE, 111:4, 722-739.

[5] EN1998 - Part 1, Eurocode 8: Design of structures for earthquake resistance - Part 1: General rules, seismic actions and rules for buildings, European Committee for Standardization (CEN), 2004/2005

[6] EN1998 - Part 3, Eurocode 8: Design of structures for earthquake resistance - Part 3: Assessment and retrofitting of buildings, European Committee for Standardization (CEN), 2004/2005

[7] EN1990 - Basis of structural design, European Committee for Standardization (CEN), 2005

[8] EN1991: Eurocode 1: Actions on structures - Part 1-1: General actions - Densities, self-weight, imposed loads for buildings, European Committee for Standardization (CEN), 2002

[9] EN1992 - Part 1: Eurocode 2: Design of concrete structures - Part 1-1 : General rules and rules for buildings, CEN, 2004/2005

[10] ETABS, Computers and Structures, Inc., 2018

[11] Ćosić, M., Folić, R., Brčić, S. (2017): "An Overview of Modern Seismic Analyses with Different Ways of Damping Introduction", Building Materials and Structures (60), Belgrade, Nr. 1, 2017, pp. 3-30; doi:10.5937/grmk1701003C

[12] Ambraseys, N., Smit, P., Sigbjornsson, R., Suhadolc, P., Margaris, B.: Internet-Site for European Strong-Motion Data, European Commission, Research-Directorate General, Environment and Climate Programme, 2002; http://www.isesd.hi.is, accessed: January 2021

[13] ORFEUS, Engineering Strong Motion Database, https://esm-db.eu/, accessed: January 2021

[14] NIST GCR 11-917-15, Selecting and Scaling Earthquake Ground Motions for Performing Response-History Analyses, NEHRP Consultants Joint Venture for U.S. Department of Commerce National Institute of Standards and Technology Engineering Laboratory Gaithersburg, Maryland, November 2011

[15] Bisch, P., Carvalho, E., Degee, H., Fajfar, P., Fardis, M., Franchin, P., Kreslin, M., Pecker, A., Pinto, P., Plumier, A., Somja, H., Tsionis, G. (2011): Eurocode 8: Seismic Design of Buildings – Worked Examples,"EC 8: Seismic Design of Buildings" Workshop, Lisbon, 10-11 Feb. 2011

[16] Mander, J., Priestley, M., Park, R. (1988): Theoretical Stress-Strain Model for Confined Concrete, Journal of Structural Engineering, Vol. 114, iss. 8, 1988, pp. 1804-1825

[17] EN1998 - Part 2, Eurocode 8: Design of structures for earthquake resistance - Part 2: Bridges, European Committee for Standardization (CEN), 2005

[18] Zhao, X., Wu, Y., Leung, A.Y.T., Lam, H.F. (2011): Plastic Hinge Length in Reinforced Concrete Flexural Members. The Twelfth East Asia-Pacific Conference on Structural Engineering and Construction, Procedia Engineering 14 (2011), pp. 1266–1274

[19] Park, R., Paulay, T. (1975) Reinforced concrete structures. New York: John Wiley & Sons; 769 pages.

[20] Priestley, M.J.N., Seible, F., Calvi, G.M.S. (1996): Seismic design and retrofit of bridges. New York: John Wiley & Sons

[21] Lađinović, Đ., Radujković, A., Rašeta, A. (2011): Seismic performance assesment based on damage of structures – Part 1: Theory*, FACTA UNIVERSITATIS, Series: Architecture and Civil Engineering Vol. 9, No 1, pp. 77 – 88, DOI: 10.2298/FUACE1101077L

[22] Ghosh, S., Datta, D., Katakdhond, A.A. (2011): Estimation of the Park–Ang damage index for planar multi-storey frames using equivalent single-degree systems, Engineering Structures, Volume 33, Issue 9, Pages 2509-2524

[23] Microsoft Excel, Microsoft Corporation

[24] EasyFit, MathWave Technologies

[25] Baker, J.W. (2015). Efficient analytical fragility function fitting using dynamic structural analysis, Earthquake Spectra, 31(1), 579-599.